

# PHENOMENA OF DISPERSION AND EXPLOSION OF HIGH PRESSURIZED HYDROGEN

Takeo, K.<sup>1</sup>, Okabayashi, K.<sup>1</sup>, Ichinose, T.<sup>1</sup>, Kouchi, A.<sup>1</sup>, Nonaka, T.<sup>1</sup>,  
Hashiguchi, K.<sup>1</sup> and Chitose, K.<sup>2</sup>

<sup>1</sup> Nagasaki Research and Development Center, MHI, 5-717-1Fukahori, Nagasaki, 851-0392, Japan

<sup>2</sup> Nuclear Energy Systems Head quarters, MHI, Minatomirai, Nishi-ku, Yokohama 220-8401, Japan

## ABSTRACT

To make “Hydrogen vehicles and refueling station systems” fit for public use, research on hydrogen safety and designing mitigative measures are significant. For compact storage, it is planned to store under high pressure (40MPa) at the refueling stations, so that the safety for the handling of high-pressurized hydrogen is essential. This paper describes the experimental investigation on the hypothetical dispersion and explosion of high-pressurized hydrogen gas which leaks through a large scale break in piping and blows down to atmosphere. At first, we investigated time history of distribution of gas concentration in order to comprehend the behavior of the dispersion of high-pressurized hydrogen gas before explosion experiments. The explosion experiments were carried out with changing the time of ignition after the start of dispersion. Hydrogen gas with the initial pressure of 40MPa was released through a nozzle of 10mm diameter. Through these experiments, it was clarified that the explosion power depends not only on the concentration and volume of hydrogen/air pre-mixture, but also on the turbulence characteristics before ignition. To clarify the explosion mechanism, the numerical computer simulation about the same experimental conditions was performed. The initial conditions such as hydrogen distribution and turbulent characteristics were given by the results of the atmospheric diffusion simulation. By the verification of these experiments, the results of CFD were fully improved.

## 1.0 INTRODUCTION

The objective of the research described here was to acquire data to be used in the reevaluation of standards in conjunction with the introduction of hydrogen refueling stations for fuel cell powered vehicles, thus serving to early practical application and popularization of fuel cells in the context of a hydrogen energy society for the future.

Storage and filling of hydrogen at a high pressure of 40MPa is planned for the hydrogen refueling stations under current consideration, and the acquisition of basic data on high-pressurized hydrogen is an urgent task. After ascertaining the properties corresponding to high-pressurized hydrogen, it will be necessary to introduce appropriate safety measures, and to review various standards and regulations so as to ensure safe operation[1][2]. The research presented here accordingly envisions various accidents associated with the storage and usage of a hydrogen refueling station, considering leakage, dispersion, and explosion behavior in the respective cases.

Representative cases involve either a pinhole occurring in equipment, resulting in continuous leakage at a constant flow volume (steady leakage), or rupture of the piping connected to the storage tanks, leading to a major leakage in a short time period (unsteady, large-scale leakage). Centered on these two cases, outdoor tests were conducted to ascertain the effects (concentration and blast pressure) of these scenarios. Results are reported below for experimental results and numerical simulation of major leakage of high-pressurized hydrogen gas occurring due to rupture of a 40MPa storage tank or the piping connected to the dispenser.

## 2.0 DISPERSION EXPERIMENTS OF HIGH-PRESSURIZED HYDROGEN

### 2.1 Experimental Apparatus and Test Field

Hydrogen refueling stations will store high-pressurized hydrogen gas at 40MPa, and outdoor diffusion-explosion tests were conducted at the Tashiro testing facility of Mitsubishi Heavy Industries in Akita

Prefecture, Japan in order to ascertain the effect of blast pressure after the leakage of high-pressurized hydrogen. The two types of conditions assumed were large-scale (unsteady) leakage from a rupture of the 10mm diameter piping connected to the high pressure storage tanks, and slight (steady) leakage from a pinhole (0.2mm~2mm in diameter). To simulate an accident, hydrogen gas was first stored in five high pressure tanks, each with a capacity of 50L, via a pressure booster. The tanks were connected to a 10mm diameter release nozzle by means of 25mm diameter piping, and a valve was fitted to the end of the piping immediately ahead of the nozzle for control of gas release. Considering the pressure loss between the high pressure tanks and the nozzle, the pressure of the hydrogen gas in the tanks was set at 65MPa to ensure a nozzle pressure of 40MPa. Assuming a large-scale leakage accident involving the rupture of 10mm diameter piping, high-pressurized hydrogen gas (40MPa) was released into the atmosphere by blow-down.

## 2.2 New Measurement Device for the Monitoring of varying Hydrogen Gas Concentration

Because it is considered that ignition timing and ignition location have great influence on the results of diffusion-explosion tests, it is important to ascertain the time-wise changes in the behavior of leaked gas. Therefore we conducted diffusion tests in advance of the diffusion-explosion tests, in order to acquire sufficient data on a time history of spatial concentration distributions for consideration of the ignition timing and ignition location with respect to explosions in large-scale, unstable leakage. However, it is difficult to measure precise hydrogen gas concentration under the unsteady state such that the distribution of dispersed hydrogen gas changes with time, because the response time of conventional gas sensors is very slow, for example 90% response time is about 7 to 8 seconds.

In order to measure more precise gas concentration, we developed a new measurement device which consists of 10 gas sensors[3]. The schematic system of the new measurement device is shown in Figure 1.

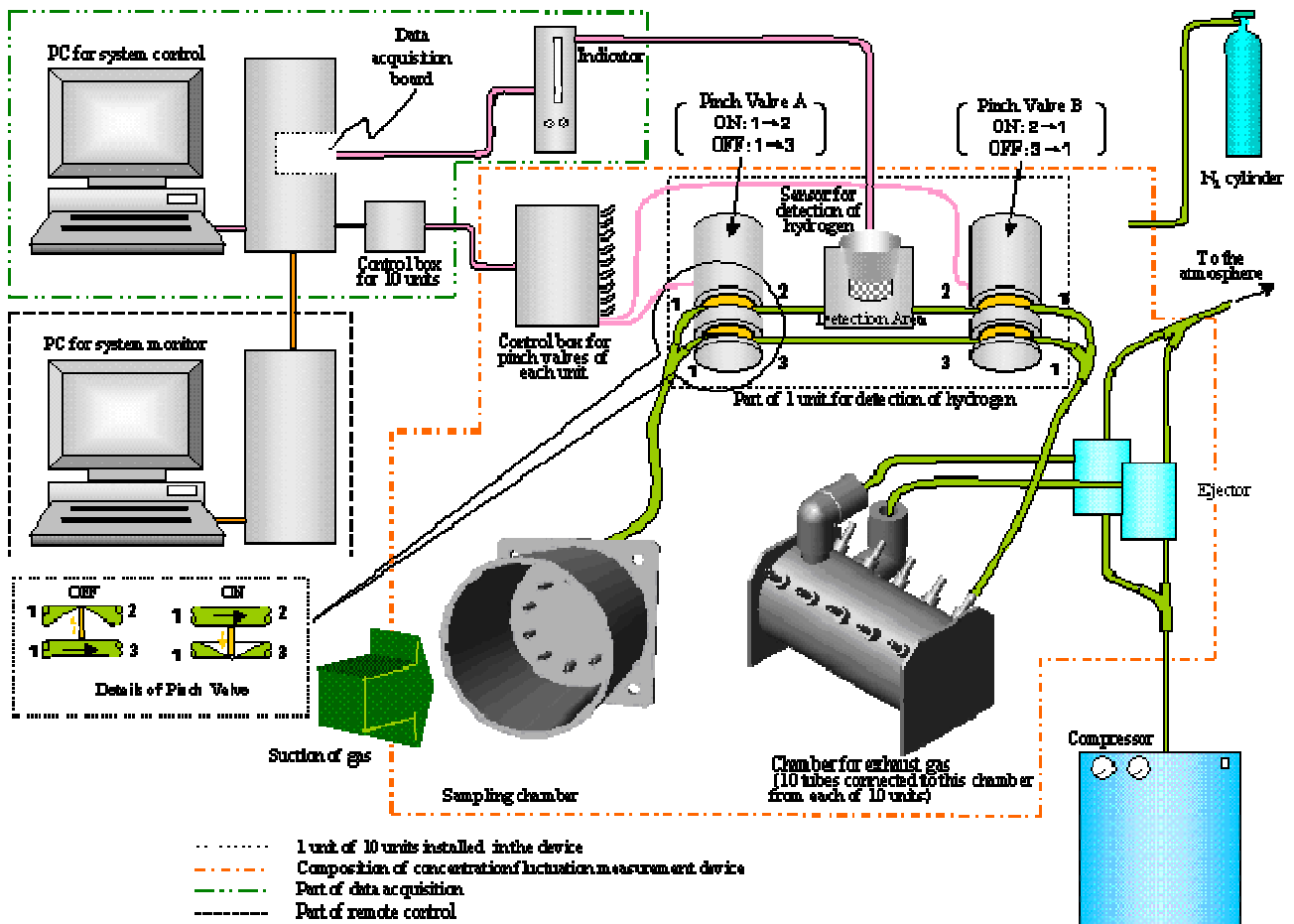


Figure 1. Schematic Illustration of Measuring System of Concentration fluctuation measurement device

It was named as concentration fluctuation measurement device, which was fabricated as shown in Figure 2 (i.e. an external view during assembly). In Figure 1, the sampling gas is led to each gas sensor every 1 second by orderly switching each flow pass which connected to the corresponding sensor. Since the sampling gas led into the sensor remains around its sensor for 10 seconds, the slow response of the sensor will be insignificant factor in precise measurement of hydrogen gas concentration. Concentration measurement, at least along the vertical cross-section, was undertaken every 1 second by using 15 units of these concentration fluctuation measurement devices.

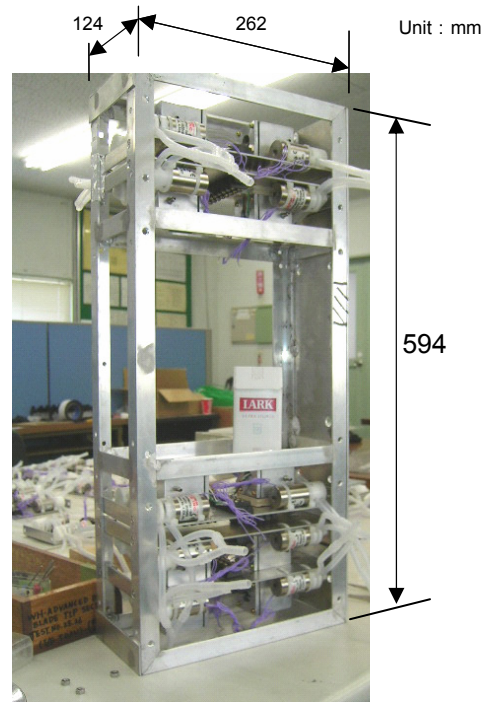


Figure 2. Concentration fluctuation measurement device

Next, in order to confirm the measurement precision of the developed device, methane gas (which can be measured rapidly) was employed, and a concentration fluctuation measurement unit was fitted with a methane gas concentration sensor (hot wire semi-conductor type with response time of 7~8s)[4]. As illustrated in Figure 3, methane gas at 2000ppm was released from the gas release nozzle A while engaging in suitable manual left-right movement, and the methane gas was sampled by means of the sampling pipe (suction tube) and the sampling port B at the same time. Concentration of the sampled gas from the sampling pipe was analyzed at 100Hz by fast response flame ionization detector HFR-400, produced by CAMBUSTION, and concentration from the sampling port B was done every 1 second by concentration fluctuation measurement device. Accordingly, in order to match with the average time of 1 second for the concentration fluctuation measurement device, data acquired at 100Hz by HFR-400 were averaged for 1 second. Figure 4 shows a comparison between values measured using the HFR400, including two types of data consisting of 100Hz and 1s average) and using the concentration fluctuation measurement device. It can be seen that the values for the concentration fluctuation measurement device are in good agreement with those for the HFR400, indicating that this device can be practically applied for the direct ascertainment of time-wise changes in the concentration of hydrogen gas.

For reference, Figure 5 presents a comparison between actual measurements of time-wise changes in concentration using a conventional concentration sensor (thermal conductivity of gases type KD-3A produced by New Cosmos Electric Company) and the concentration fluctuation measurement device. Measurement using both types of equipment was performed simultaneously at essentially the same location. Although it was physically impossible to place both pieces of equipment at exactly the same location, the

location-induced discrepancy is considered to be slight, and it can be seen that a major improvement was achieved in terms of responsiveness.

Gas to be measured	CH <sub>4</sub>	H <sub>2</sub>
Type of gas sensor	Hot wire semi-conductor	Thermal conductivity of gases
Response time	6~7 seconds	7~8 seconds

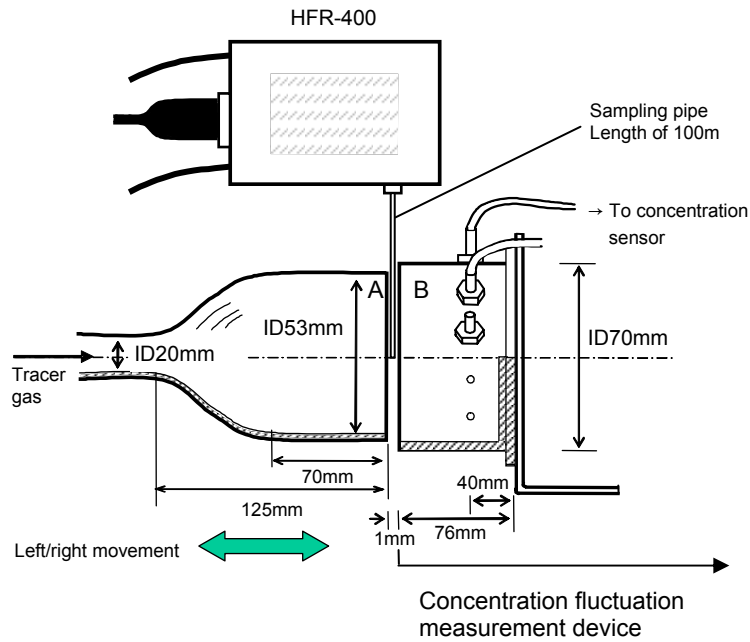


Figure 3. Verification test procedure for the concentration fluctuation measurement

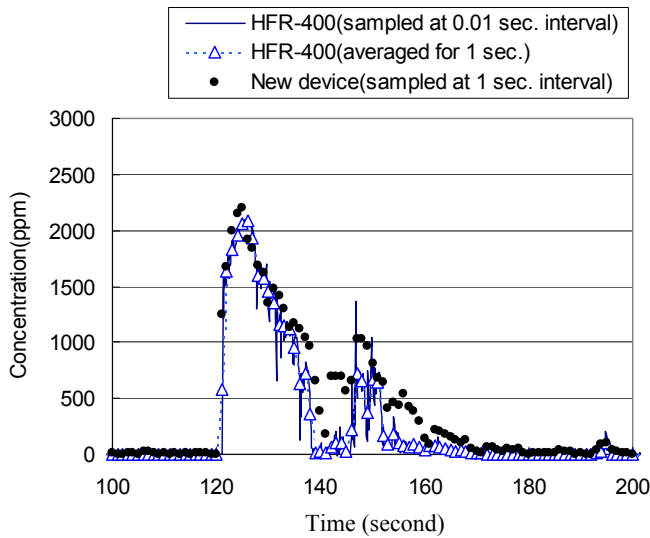


Figure 4. Verification of concentration fluctuation measurement device

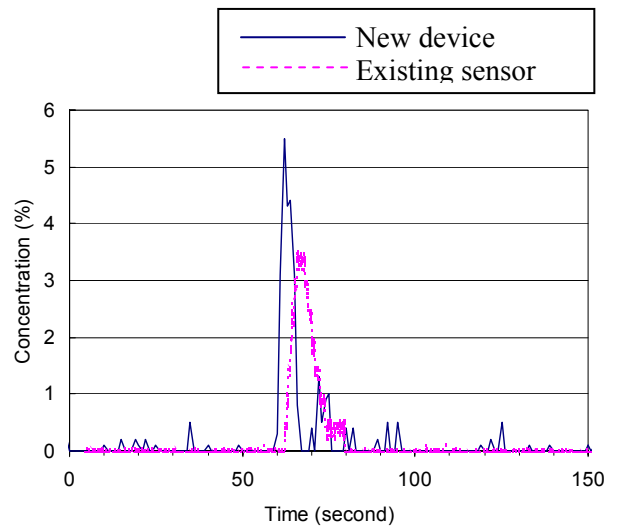


Figure 5. Comparison of response of measurement devices

### 2.3 Results of the Experiments

Hydrogen gas consisting of 250 liter at 40MPa (approx.  $100\text{Nm}^3$ ) was released from the 10mm diameter nozzle into the atmosphere by means of blow-down. Atmospheric conditions at this time were nearly calm (average wind direction of WNW, wind speed of  $0.2\text{m/s}$ ). Time-wise changes in the concentration distribution within the vertical cross-section along the jet flow axis were measured using 15 units of the concentration fluctuation measurement device, as summarized in Section 2.2. At downwind distance  $X < 8\text{m}$ , however, hydrogen gas has high momentum as it jets out under high pressure, and the jet flow may impact on the measurement equipment itself. Accordingly, measurement was not conducted within this area.

Figure 6 presents the concentration measurement results. With the elapse of 1second following leakage, although the dispersion range of the gas tended to gradually become smaller at the leading edge, the high concentration region of over 10% extended for over 10m, and this was found to be maintained until after the elapse of 5 second from leakage. Based on these results, ignition timing was varied from approx. 1 second to 5 second after leakage, and the ignition location was varied within a range of 7.5m from the leakage origin in consideration of test equipment constraints.

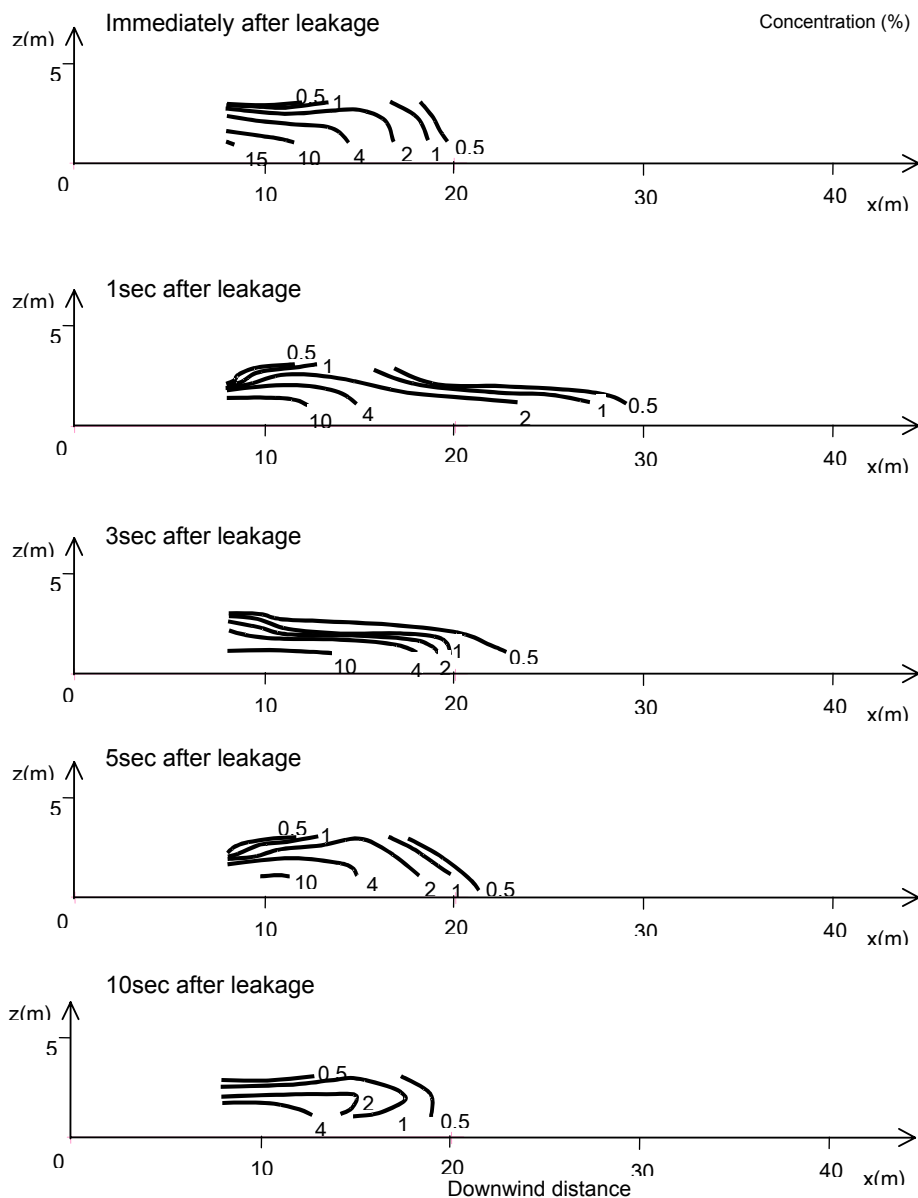


Figure 6. Time history of concentration contour

### 3.0 EXPLOSION EXPERIMENTS OF HIGH-PRESSURIZED HYDROGEN

#### 3.1 Apparatus and the Method of the Experiment

Measurements were made in terms of pressure waves, radiant heat, ion current (detection of flame front), and imaging (400f/s high speed video, 50f/s normal video, and 50f/s UV video), with locations indicated in Figure 7. Ignition was intentionally performed with a continuous electric spark set along the disperse axis at 0.5~7.5m away from the nozzle.

Because frequency characteristics are particularly important in pressure wave measurement, piezzo electric type (Kulite, resonant frequency > 150KHz) pickups were used, the reliability of which have been demonstrated in past explosion tests, as well as microphone type (B&K, resonant frequency > 140KHz) pickups for remote positioning over 50m away. Gauge amps and preamps were positioned within 5m of the pickups. The data recorder (12bit, with sampling rate of 10MHz) was placed at the relay point as shown in Figure 7, and was operated through a connection with a LAN cable from the control bunker about 300m away. The actual ignition timing was determined using a photo-sensor facing the ignition point.

Test parameters consisted of the following four items:

- (1) Leakage opening (nozzle diameter (d) of 0.5~25mm)
- (2) Time elapsed from start of leakage to spark ignition (ting=0.5~20s)
- (3) Tank capacity and initial pressure (25~100Nm<sup>3</sup>, Po=10~40MPa)
- (4) Ignition location (distance from the leakage nozzle to the spark plug; Xign=0.5~7.5m)

The reason for varying the capacity of the hydrogen tank subject to leakage is that, the tank pressure and flow volume decrease with time elapsed following leak initiation, especially in the case of d=5mm or greater. It is thus considered that the premixture volume and concentration (relating to explosiveness) are dependent upon the tank capacity.

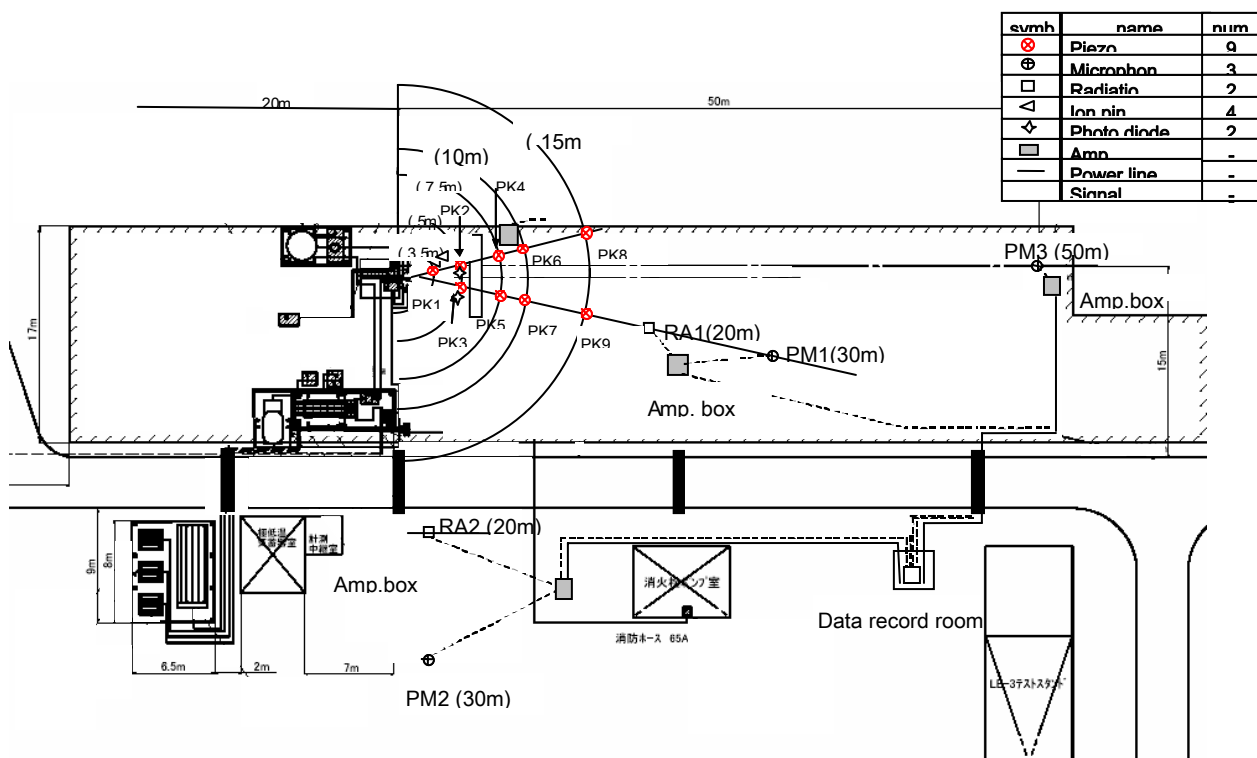


Figure 7. Arrangement of gauges and sensors for hydrogen explosion and diffusion flame experiments

## 3.2 Results and Discussion

### (1) Explosion characteristics and mechanism

Figure 8 shows a typical pressure waveform, while Figure 9 indicates the relation between maximum over-pressure ( $\Delta P$ ) and distance ( $L$ ) when ignition timing ( $t_{ign}$ ) was varied. This waveform, the pressure recession properties, and the effects of varying  $t_{ign}$  were accompanied by the following characteristics, previously not observed in explosion tests conducted by igniting static premixture in a chamber.

- <1> The rise in the pressure wave is extremely rapid in terms of deflagration. Also, the reduction in pressure at 10~15m distant from the ignition point is slight; under conditions of  $t_{ign}=2s$ ,  $\Delta P > 15kPa$ , indicating the measurement of extremely high pressure in the near field. Following the peak in initial maximum pressure, a low pressure wave was sustained, corresponding to the after-burn of the hydrogen that continued to be released subsequent to ignition.
- <2> Under the conditions presented in Figure 8, average flame propagation velocity was about  $3.9m/12ms = 325m/s$ . Under open space conditions, with no obstacles to encourage flame turbulence, the flame propagation velocity rose to over  $300m/s$  at a distance of approx. 4m. This is thought to be due to the initial turbulent mixing resulting from the high pressure jet, with strong turbulent premix combustion occurring immediately after ignition. However, the premixture configuration was cylindrical, with rapid recession of the pressure wave over distance (i.e., distance to an exponent of about -1.5).
- <3> According to the dispersion experiments shown in Figure 6 and numerical simulation, concentrations of over 10% and over 4% lead to maximum premixture volumes at 3s and 7s after leakage, respectively. However, as shown in Figure 9, the earlier the ignition timing following leakage, the greater the maximum over-pressure tended to be. This indicates that leakage velocity (turbulent energy) has a greater effect on explosiveness than does the total amount of leakage or the premixture volume.

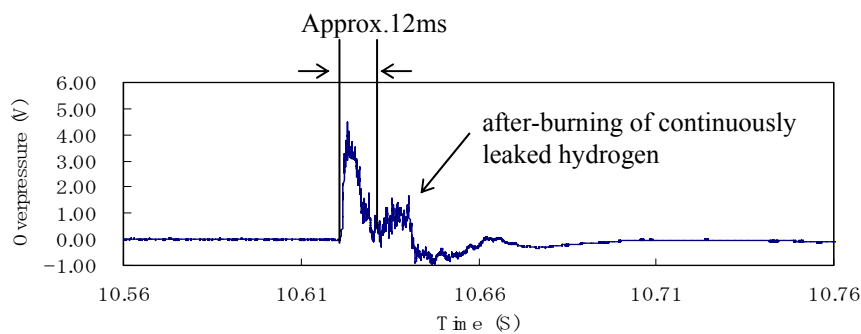


Figure 8. Typical pressure wave at 3.9m away from ignition point ( $P_0=40MPa$ ,  $d=10mm$ ,  $t_{ign}=2s$ )

### (2) Effect of protection wall

A concrete barrier 3m high and 6m wide simulating a protection wall was positioned 6m from the nozzle, and the effect of a protection wall on explosions was investigated. Figure 10 shows an example of the results (relation between  $\Delta P$  and  $L$ ), comparing the situation with and without such a protection wall.

Use of the protection wall promoted gentle attenuation of  $\Delta P$  with respect to  $L$ , the relation was observed to be an exponent of about -1. This is considered to be due to collision of the hydrogen jet with the wall surface, with premixture accumulation on the inside of the wall immediately prior to ignition, thus resulting in the loss of directionality in the propagation of the waveform. This is the same as the relation between pressure and distance when a premixture is introduced into a spherical chamber and ignited at the center.

Also, the absolute value of maximum over-pressure receded from about 12kPa without the wall to about 7kPa behind the wall (at L=10m), but these converged to about 3kPa at 40m distant. That is, pressure is substantially reduced immediately behind the protection wall, but the wall has almost no effect in the far field where the pressure has decreased.

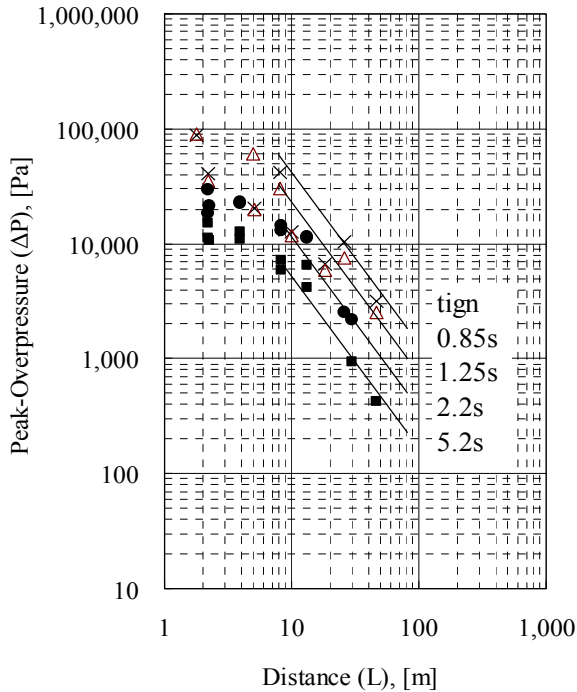


Figure 9. Effects of ignition delay ( $t_{ign}$ ) on the peak overpressure ( $P_0=40\text{MPa}$ ,  $d=10\text{mm}$ ,  $X_{ign}=4\text{m}$ )

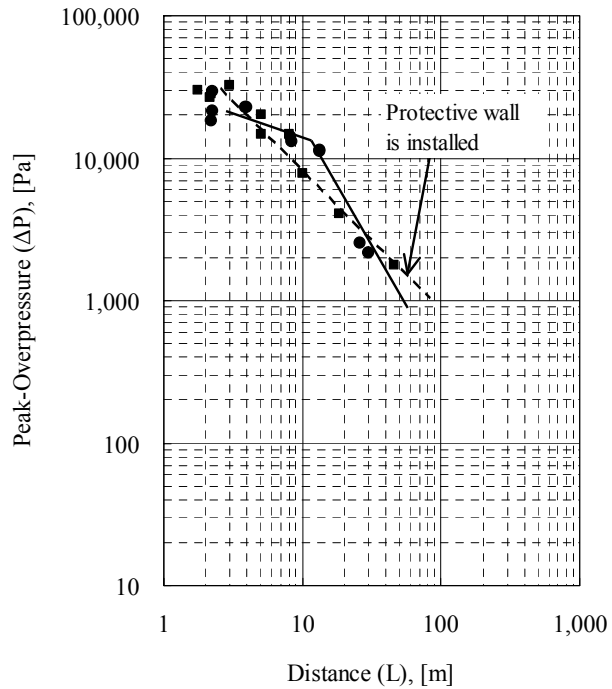


Figure 10. Effects of protective wall on the pressure wave propagation ( $P_0=40\text{MPa}$ ,  $d=10\text{mm}$ ,  $t_{ign}=2\text{s}$ ,  $X_{ign}=4\text{m}$ )

### (3) Effect of leakage opening diameter

Figure 11 presents the results for variance of the nozzle opening diameter when the jet pressure from the nozzle was held constant at 40MPa. In the case of  $d=5\text{mm}$  and under, the small flow volume means that the jet pressure is nearly constant, such that the flow volume is proportional to the nozzle cross-sectional area (i.e., proportional to the square of the nozzle diameter  $d$ ). The flow volume differed by a factor of 6.3 times for diameters of 5mm and 2mm, while the factor was approx. 5 times with respect to  $\Delta P$ . Flow volume differed by a factor of 4 times for diameters of 2mm and 1mm, with  $\Delta P$  differing by a factor of 3.5 times. Accordingly, at 40MPa and in the nozzle opening diameter range of 1~5mm, flow volume and  $\Delta P$  exhibit essentially proportional relationships.

The relation between jet flow volume and maximum over-pressure was then reviewed over a wide range of test conditions. Because flow volume is extremely high for a large opening of 10mm, pressure decreases with the time elapsed from release. Figure 12 shows the calculation results for the variation of leakage rate with time. Figure 13 indicates the calculated relation between jet flow volume at the instant of ignition and  $\Delta P$ , and it can be seen that both are essentially proportional. It is considered that explosiveness is more dependent upon flow volume at the time of ignition than on the total volume of leakage, i.e., largely dependent upon turbulent mixing energy at the time of ignition.



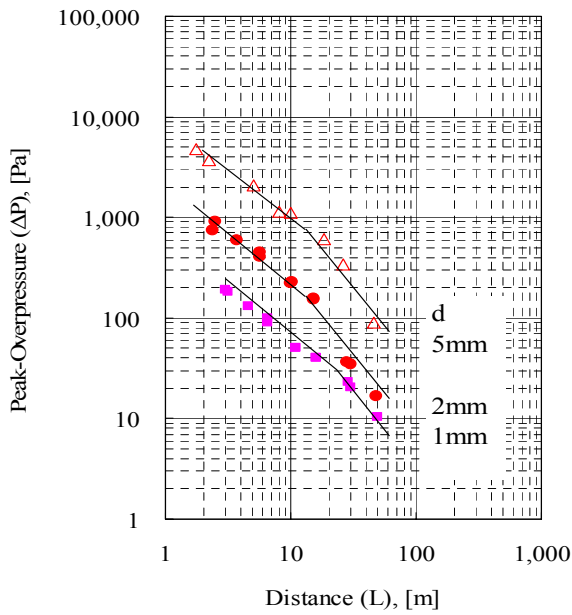


Figure 11. Effects of nozzle diameter (d) on the peak overpressure  
( $P_0=40\text{MPa}$ , leakage rate is constant with time)

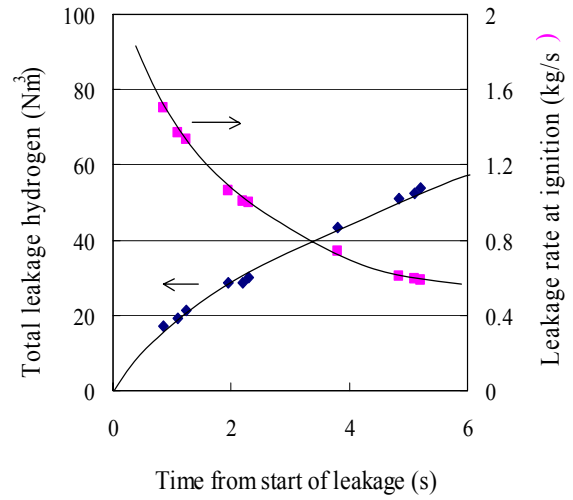


Figure 12. Variation of calculated hydrogen leakage rate with time  
(Initial storage amount= $100\text{Nm}^3$ ,  $d=10\text{mm}$ )

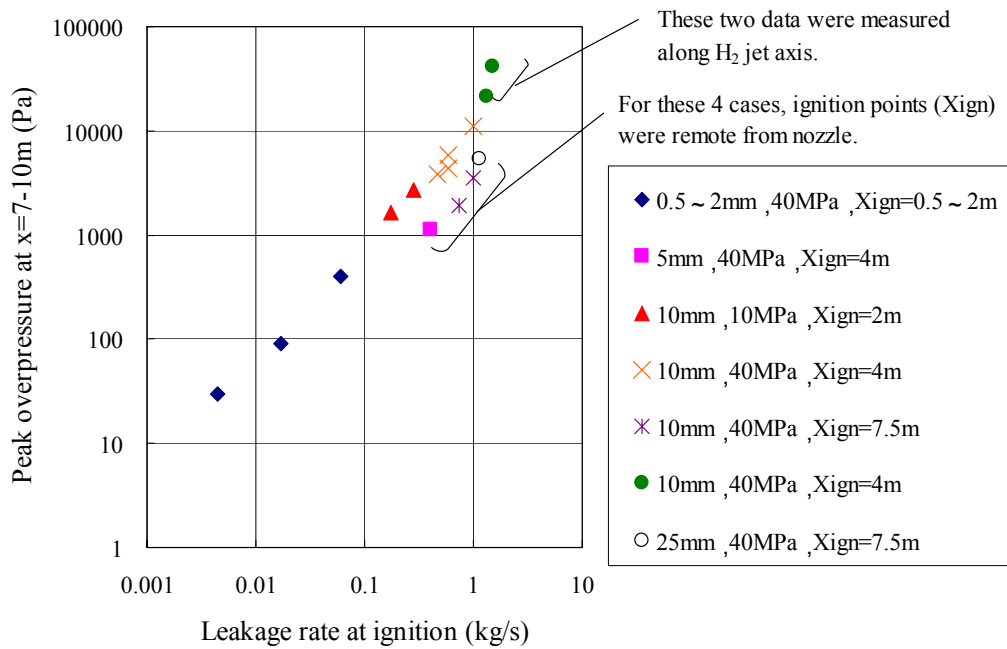


Figure 13. Relationship between experimentally obtained peak overpressure and leakage rate

### 3.3 Numerical Simulation of Hydrogen Explosion

Numerical calculations were performed for each compressible conservation formula (turbulent flow corresponding to the  $k-\epsilon$  model), with chemical reaction speed reflected in the turbulent combustion speed ( $St$ ) indicated below, and with the heat generated with respect to combustion velocity occurring at the flame surface. Here,  $S_t$ ,  $S_l$ ,  $u'$ , and  $L_t$  express turbulent combustion velocity, laminar combustion velocity, the velocity fluctuation component, and the scale of turbulence[5][6].  $R_c$  represents the consumption speed of the fuel per unit volume, while  $D_f$  is the turbulent diffusion coefficient.

$$S_t = 1.8u'^{0.412} L_t^{0.196} S_{ll}^{0.784} \nu^{0.196}$$

$$S_{ll} = S_l(1 + F_c R_f)$$

$$R_c = -T_c \cdot \rho \cdot \frac{S_t^2}{D_f} \cdot \min[m_{fu}, m_{O_2}/s, m_{pr}/(1+s)]$$

$T_c$  and  $F_c$  are constants specific to the fuel as regulated by  $St$ , with values employed as determined from analysis on explosion test results for hydrogen-air premixtures undertaken by the SRI International-Poulter Laboratory [7].

First, the concentration, velocity, and temperature distributions were determined for the premixture formed in the gas phase, based on compressible fluid calculations, and explosion calculations were performed taking these as the initial conditions. In the case of high pressure leakage, where initial turbulence properties are particularly significant, it is important to apply the above characteristics (e.g., the fluctuation velocity component obtained from fluid calculations, and the scale of turbulence) to the turbulent combustion model. Figure 14 presents the relation between the pressure wave measurement and calculation results, and it can be seen that the pressure rise properties and maximum values are well reproduced. Figure 15 shows the relation between distance and maximum over-pressure, and it can be seen here that both are in good agreement. During tests, in order to avoid collision of the jet flow with the sensors, pressure was measured along a line offset by about 20 degrees from the jet flow center axis, but pressure along the center axis were obtained from calculations. As a result, pressure along the center axis was found to be about 1.5 times, and is predicted to reach a maximum of about 20kPa under initial conditions of  $P_0=40\text{MPa}$ ,  $d=10\text{mm}$ , and  $t_{ign}=5\text{s}$ .

Next, prediction at full scale (storage volume of  $800\text{Nm}^3$ ) was undertaken using the constructed simulation. Initially, the state of the combustible premixture forming a gas phase due to leakage from a 10mm opening at 40MPa was obtained from diffusion calculations. It was thus determined that maximum dispersion would be reached at 13.7s for a hydrogen concentration of under 4%, or at 5.5s for a concentration of under 10%. Explosion simulations were then conducted for these two cases (Figure 16). As a result, it was found that maximum over-pressure was about 300kPa along the center axis of jet flow, with maximum impulse of 700Pa.s, and with strong directionality. Along the axis 30 degrees offset from the center axis, maximum over-pressure and maximum impulse declined to about 30kPa and about 200Pa.s respectively.

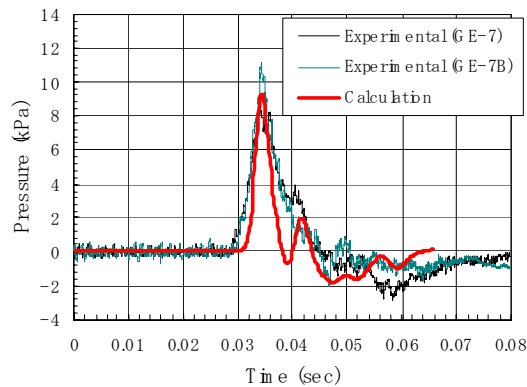


Figure 14. Comparison between experimental and calculated pressure wave  
( $P_0=40\text{MPa}$ ,  $d=10\text{mm}$ ,  $t_{ign}=5\text{s}$ ,  $x=6\text{m}$ )

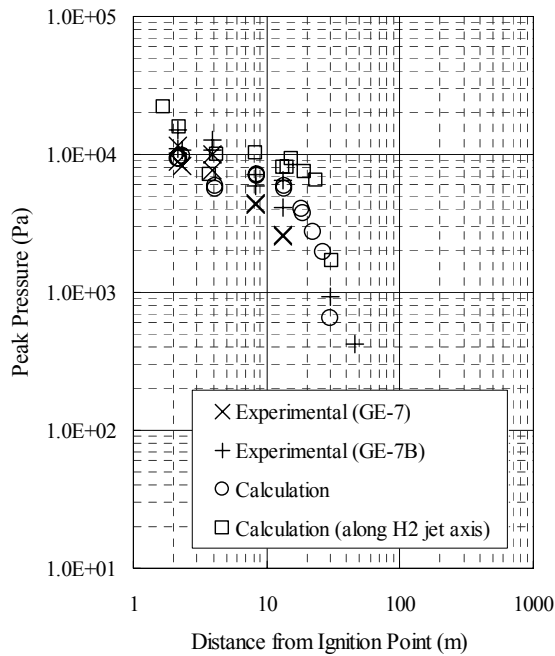


Figure 15. Comparison between experimental and calculated Overpressure.  
 $(P_0=40\text{MPa}, d=10\text{mm}, \text{tign}=5\text{s})$

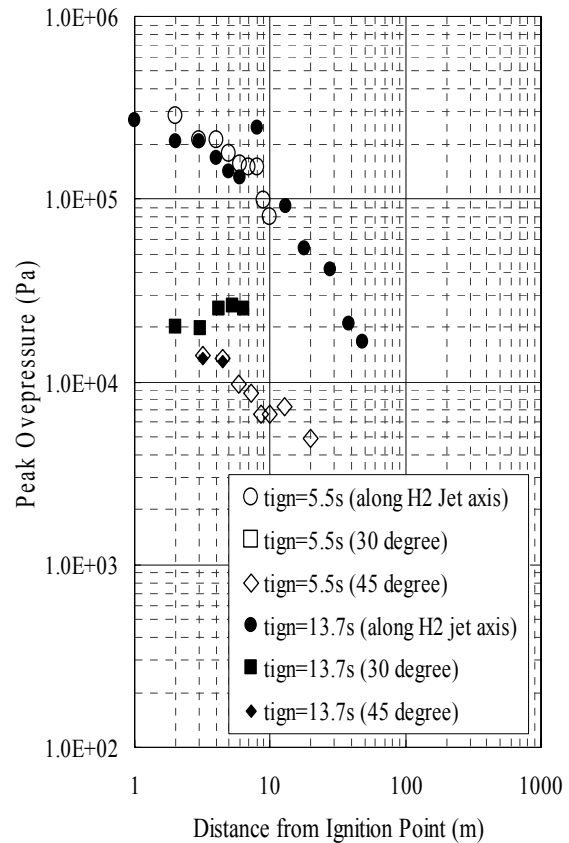


Figure 16. Calculation for practical scale  
 $(800 \text{ Nm}^3 \text{ hydrogen storage})$   
 $(P_0=40\text{MPa}, d=10\text{mm},$   
 $\text{tign} : \text{calculation parameter})$

#### 4.0 CONCLUSIONS

Data was acquired from outdoor experiments on the dispersion and explosion characteristics of high-pressurized hydrogen gas with an initial pressure of 40MPa leaked into the atmosphere from a piping rupture (opening of 10mm in diameter). Concentration fluctuation measurement device was proposed in order to ascertain time-wise changes in the dispersion state of leaked hydrogen gas. After verifying the measurement precision of this device, it was employed to measure time-wise changes in the concentration distribution of the vertical cross-section along the axis of jet flow. In the explosion tests, post-leakage ignition location and timing were varied, and blast pressure data was obtained. The results indicated that, explosive was strongly dependent on the turbulent flow from high pressure leakage. Simulations reflecting these factors were performed for high-pressurized hydrogen gas, and pressure waveforms were reproduced. Using the experimental and simulation results thus obtained, the comprehensive prediction method will be established by combining both hydrogen dispersion and explosion behaviors under various configuration and leakage conditions in the future. It will also be possible to quantitatively ascertain the risk associated with hydrogen refueling stations, by analyzing the mechanisms of occurrence for accident phenomena and their frequency. The consequence of each accident scenario is obtained by these evaluation results. Furthermore, these results can then be utilized for the reduction of the risk associated with facilities that handle high-pressurized hydrogen gas, and for the consideration of safety measures.

## ACKNOWLEDGEMENTS

This research was undertaken as part of “Development for Safe Utilization and Infrastructure of Hydrogen” sponsored by NEDO (the New Energy and Industrial Technology Development Organization). The authors would like to extend their thanks for guidance and support to NEDO, the Japan Petroleum Energy Center and The Institute of Applied Energy.

## REFERENCES

1. Iwai, Y., Japan's Approach to Commercialization of Fuel Cell/Hydrogen Technology, Proceedings of 15<sup>th</sup> World Hydrogen Energy Conference, June 2004, Yokohama Japan.
2. Hayashi, T., et al., Hydrogen Safety for Fuel Cell Vehicles, Proceedings of 15<sup>th</sup> World Hydrogen Energy Conference, June 2004, Yokohama Japan.
3. Okabayashi, K., et al., Research and Development on the Phenomena of Dispersion of High-Pressurized Hydrogen Gas and Liquefied hydrogen, Proceedings of the 18th Annual Meeting of Japan Petroleum Energy Center, 10-11 May 2004, Tokyo, in Japanese.
4. Takeno, K., et al., On the Phenomena of Dispersion and Explosion of High-Pressurized Hydrogen Gas, Proceedings of the 24th Annual Meeting of Hydrogen Energy Systems Society of Japan, 10-11 December 2004, Saitama, in Japanese.
5. Catlin, C. A. and Lindstedt, R. P., Premixed Turbulent Burning Velocities Derived from Mixing Controlled Reaction Models with Cold Front Quenching, *Combustion and Flame*, vol.85, pp.427 (1991).
6. Bray, K.N.C., *Turbulent Reacting Flows*, Topics in Applied Physics, Springer Verlag, Berlin (1980).
7. Takeno, K., et al., On the Phenomena of Dispersion and Explosion of High-Pressurized Hydrogen Gas, Proceedings of the 24th Annual Meeting of Hydrogen Energy Systems Society of Japan, 10-11 December 2004, Saitama, in Japanese.
8. Takeno, K., et al., Study on dispersion and explosion phenomena of gaseous hydrogen leakage under high-pressurized condition, Proceedings of the 23th Annual Meeting of Hydrogen Energy Systems Society of Japan, 5-6 December 2003, Tokyo, in Japanese.